Age constraints of reduction spot formation from Permian red bed sediments, northern Switzerland, inferred from U-Th-Pb systematics

Autor(en): **Hofmann, Beda A. / Frei, Robert**

Objekttyp: **Article**

Zeitschrift: **Schweizerische mineralogische und petrographische Mitteilungen = Bulletin suisse de minéralogie et pétrographie**

Band (Jahr): **76 (1996)**

Heft 2

PDF erstellt am: **08.08.2024**

Persistenter Link: https://doi.org/10.5169/seals-57700

SCHWEIZ. MINERAL. PETROGR. MITT. 76, 235–244, 1996

Age constraints of reduction spot formation from Permian red bed sediments, northern Switzerland, inferred from U–Th–Pb systematics

by *Beda A. Hofmann*[1] and *Robert Frei*[2]

Abstract

Uranium is commonly concentrated in the core (dark centre) of small-scale (1 to 10 cm diameter) chemically reduced spheroidal rock volumes (reduction spots) in red bed sediments. The U–Th–Pb relations of reduction spots from Permian red beds of northern Switzerland were investigated. U–Pb data of 17 samples from 12 reduction spots and their host rocks selected from the Kaisten, Riniken and Weiach boreholes reveal that Pb and U, including short lived ^{238}U daughter elements, were mobile during and after formation of the spots. Th was mobilized only very locally. Bleached haloes around mineralized cores are depleted in Pb by 60 ± 10% compared with bulk rocks. Less than 5% of the mobilized Pb re-accumulated in the cores. U-rich cores of reduction spots do not yield meaningful U–Pb ages due to significant mobilization of short-lived daughters of ^{238}U and of radiogenic Pb. Ages calculated from microprobe analyses of selected large grains of uraninite from reduction spot cores form two probability maxima at 138 Ma (Jurassic/Cretaceous) and 45 Ma (Tertiary). The age of reduction spot formation is believed to correspond to the former probability maximum while the latter may represent a remobilization event in the Tertiary. Two pairs of host rock and halo yield a ^{232}Th–^{208}Pb isochron age of ≥ 105 ± 12 Ma and demonstrate the feasibility of Th–Pb dating of red bed bleaching phenomena. Formation of reduction spots in northern Switzerland appears to have occurred during the Lower Cretaceous (100 to 140 Ma), corresponding to a sedimentary cover of at least 1000 m.

Keywords: red beds, Permian, reduction spots, U–Th–Pb systematics, daughter element loss, northern Switzerland.

1. Introduction

1.1. GENERAL FEATURES OF REDUCTION SPOTS

Small-scale (1 to 10 cm diameter), spheroidal, chemically reduced volumes (reduction spots, see Fig. 1), are present in red beds of different age in many parts of the world (e.g. MAW, 1868; CARTER, 1931; PERUTZ, 1940; TANTON, 1948; MEMPEL, 1960; HARRISON, 1975; CURIALE et al., 1983; HOFMANN, 1990, 1991a). Reduction spots consist of a dark, mineralized core often surrounded by a pale halo. The near-spherical shape in consolidated red bed clays indicates that their formation largely postdated compaction. Enrichments of rare elements – predominantly U, V, As, Ni, Co, Pb, Cu and Se – generally occur in the millimetre to centimetre sized centres of the reduction spots (MEMPEL, 1960; HARRISON, 1975; HOFMANN, 1991a). Most enriched elements occur as discrete, usually very fine-grained minerals (Fig. 2) impregnating a host rock matrix. The haloes are depleted in Fe. Reduction spots are the result of local, small-scale, diffusion-controlled redox processes operating in red beds. The identity of the reductants involved is uncertain, but the existence of a mobile, kinetically inert reductant which is converted at discrete sites of catalysis is considered to be likely (HOFMANN, 1991a, 1992). Formation of reduction spots strongly depends on temperature which is related to depth of burial and, therefore, age of formation. Dating such features is an important step towards an understanding of their formation mechanisms.

First attempts to dating reduction spots from northern Switzerland based on chemical (micro-

[1] Naturhistorisches Museum, Bernastrasse 15, CH-3005 Bern, Switzerland. E-mail: hofmann@nmbe.unibe.ch
[2] Gruppe Isotopengeologie, Mineralogisch-petrographisches Institut, Erlachstrasse 9a, CH-3012 Bern, Switzerland. E-mail: robert@mpi.unibe.ch.

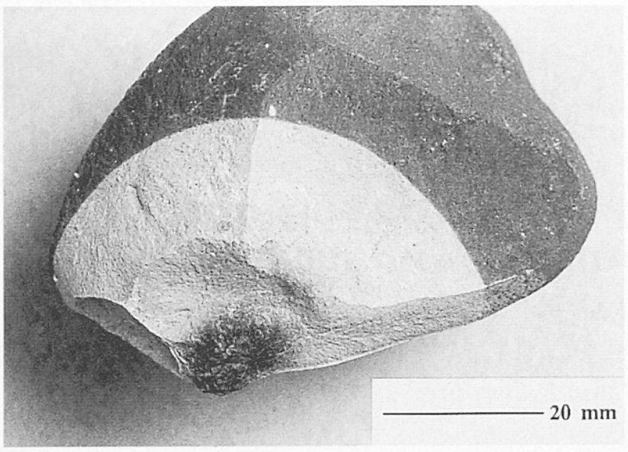

Fig. 1 Typical reduction spot in Permian red bed claystone from northern Switzerland (Kaisten drill hole, 214.9 m depth).

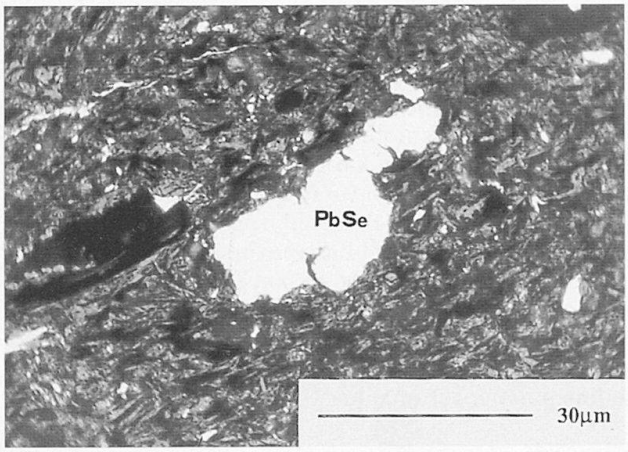

Fig. 2 Photomicrograph of a mineralized reduction spot core (Kaisten, 214.9 m) showing the extremely fine-grained nature of uranium minerals (grey) intergrown with clay matrix (black) and the intimate association of uranium minerals with clausthalite (PbSe). Reflected light, oil immersion.

probe) U–Pb analyses, K–Ar dating and compaction estimates yield Cretaceous and Jurassic ages (HOFMANN, 1990). K–Ar roscoelite ages of 112 ± 2, 173 ± 2 and 190 ± 2 Ma may be influenced by inherited detrital components and should be regarded as maximum ages. Uranium series investigations show that samples at depth are in secular equilibrium (HOFMANN, 1991b), indicating that no significant deposition or removal of U occurred during the last 0.5 Ma.

1.2. OBJECTIVE OF THIS STUDY

The objective of this study was to obtain an accurate age of reduction spot formation in northern Switzerland. As shown in this work, however, the U–Pb system in mineralized cores of reduction spots proves unsuitable for obtaining formation ages. Nevertheless, U–Th–Pb systematics yield insight into the processes of reduction spot formation and diagenetic redox processes in general and can be used to obtain a ^{232}Th–^{208}Pb minimum age of halo formation.

1.3. PROBLEMS ENCOUNTERED WHEN DATING FINE-GRAINED U-MINERALS

Attempts to date fine-grained uranium minerals from sediment-hosted mineralizations commonly result in inaccurate ages or even fail because closed system requirements were not met (LUDWIG et al., 1982; LUDWIG et al., 1984; LUDWIG and SIMMONS, 1992). Diagenetic uranium minerals such as coffinite, uraninite and brannerite commonly are extremely fine-grained. Several processes of daughter element loss from fine-grained minerals are possible: alpha recoil, recrystallization due to Ostwald ripening, leaching from damaged lattice sites, and metamictization (coffinite and brannerite). Because the intermediary daughters of ^{238}U have half-lives much longer than those of the ^{235}U decay series, mobility of intermediary daughters may affect ^{238}U–^{206}Pb ages to a greater extent. Strongly discordant U–Pb ages and abnormally high $^{207}Pb/^{206}Pb$ ratios suggest ^{238}U series mobility. Because loss of ^{226}Ra (relatively long half life, mobility) and ^{222}Rn (highly mobile) is most likely, radioactive equilibrium may be retained between ^{230}Th, ^{234}U and ^{238}U as observed in deep-seated reduction spots from northern Switzerland (HOFMANN, 1991b). In addition to the small size of individual grains of U minerals which results in a large specific surface area, the volume of U mineralized rock (typically 1 cm^3 or less) is small which renders this type of samples particularly susceptible to open-system behaviour.

2. Geologic setting, samples and techniques

2.1. GEOLOGIC SETTING OF THE PERMIAN IN NORTHERN SWITZERLAND

The geologic setting and sedimentology of the Permian of northern Switzerland has been described by MATTER (1987). Reduction spots are present in coarse-grained alluvial fan sediments and playa mudstones. Permian red beds as well as Permian and Carboniferous organic-rich sediments are located in a complex graben structure in the crystalline basement (DIEBOLD et al., 1992).

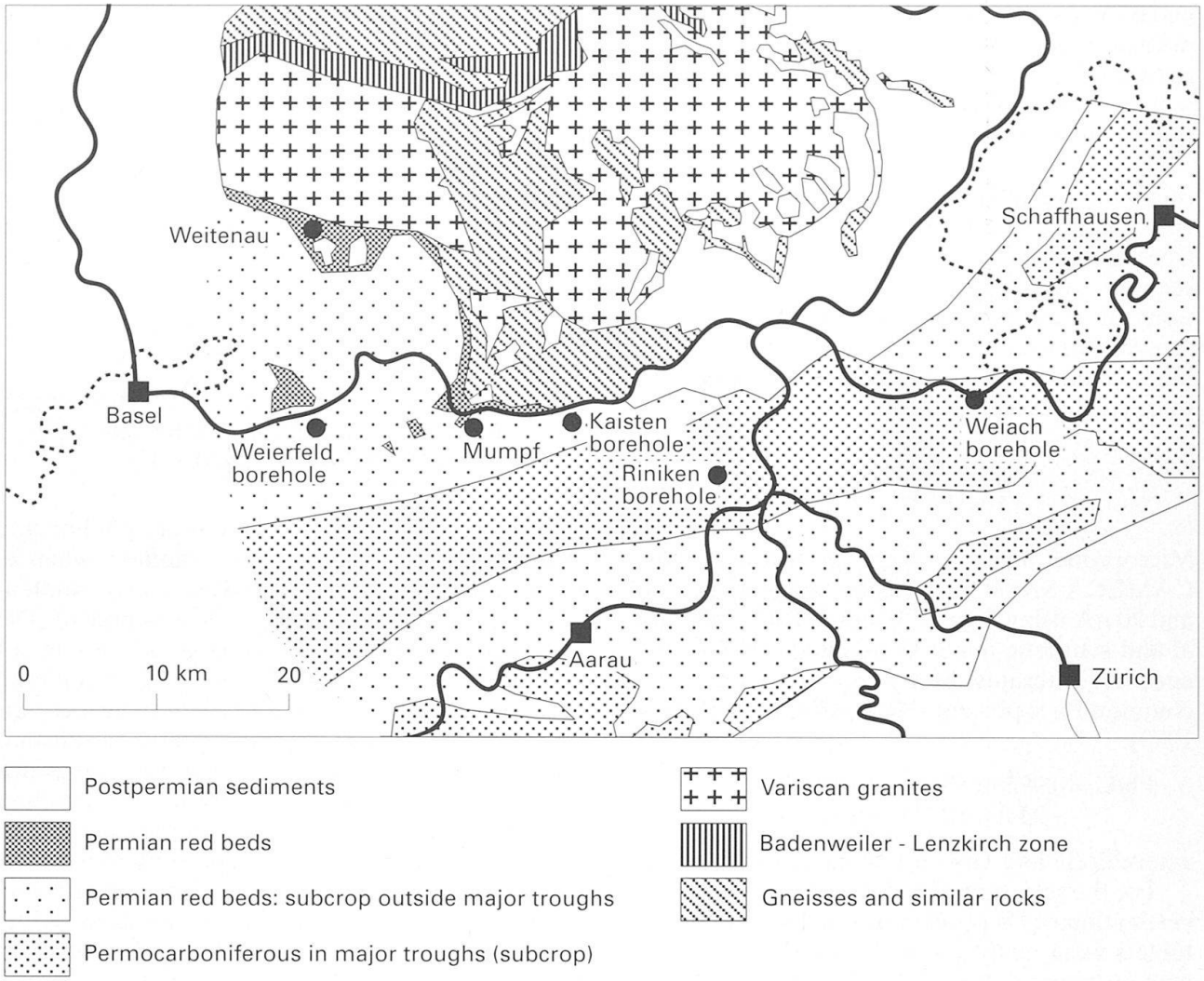

Fig. 3 Sketch map showing subcrop and outcrop of Permian red bed sediments in northern Switzerland and adjoining southern Germany. Also shown is the Schwarzwald crystalline complex.

The Permian red beds are overlain by 800 to 1000 m of Mesozoic and up to several 100 m of Tertiary and Quaternary sediments. The maximum depth of burial thus varies from about 1500 to 2500 m.

The present study employing microprobe- and isotopic techniques is based on samples taken from the Kaisten, Weiach and Riniken boreholes, located at different positions in the Permocarboniferous graben in central northern Switzerland (Fig. 3). These boreholes were drilled in the years 1983–1984 as part of a regional investigation program by Nagra (Swiss National Cooperative for Radioactive Waste Disposal). The geology of these drill holes was described in detail by MATTER et al. (1988 a, b) and PETERS et al. (1989). Permian red beds were intersected at a depth ranging from 125 to 297 m (Kaisten), 816 to 1801 m (Riniken) and 991 to 1170 m (Weiach). Reduction spots are abundant in drill cores from each of the above mentioned boreholes (HOFMANN, 1990). One sample (Kai 351) was taken from a reduction spot located in altered gneiss just below the base of Permian sediments. Microprobe analyses were additionally performed on samples from Permian mudstones from the Weierfeld borehole (drilled in 1875) near Rheinfelden, Switzerland (Fig. 3).

2.2. SAMPLES

Samples of drill cores containing reduction spots were selected from Nagra's core depot. Samples of U-rich reduction spots were identified using a Geiger counter. Mineralized cores from each reduction spot were gently crushed and fragments of a few milligrams weight were selected for U–Pb analysis by comparing U and Pb peak heights in XRF scans to avoid sampling Pb-rich portions of the spots. U-rich subsamples were further identi-

fied by means of qualitative radioactivity ($\alpha + \beta + \gamma$) measurements. Due to the extremely fine-grained nature of the U-minerals and their intergrowth with other minerals it was not possible to obtain pure mineral separates for analysis.

U–Th–Pb systematics investigations of host rocks, bleached haloes and clausthalite (PbSe) in cores were carried out on two reduction spots from Kaisten (Kai 208.6 m , Kai 214.9 m). Polished sections were prepared from representative sections of each mineralized core for optical microscopy and electron microprobe analysis of uranium minerals for U, Th and Pb with the objective to calculate chemical ages.

2.3. TECHNIQUES

Microprobe analyses were performed with a CAMECA SX-50 microprobe operated at 15 kV and 20 nA using U and Pb metal, ThO_2 and natural and synthetic minerals as standards. Chemical ages were iterated with the assumption that no common Pb is present (HOFMANN, 1989; BOWLES, 1990):

$$Pb/U = 0.9928(e^{\lambda 238 * t} - 1) + 0.0072(e^{\lambda 235 * t} - 1) + \\ + Th/U(e^{\lambda 232 * t} - 1)$$

where Pb/U and Th/U are molar ratios.

For the selection of whole rock samples and investigation of Pb geochemical behaviour, powder tablets were analyzed for U, Th and Pb by XRF with an error of about 10% at the 10 ppm level. In some samples, Pb concentrations determined by XRF were checked by AAS and found to be in close agreement. Th was determined by ICP-MS using a Na_2O-sinter decomposition method by XRAL laboratories with a stated error of 2%.

In the host rocks of the reduction spots total Pb was analyzed using a HCl–HNO_3-decomposition method. Labile Pb was analyzed in leachates obtained by cold leaching of rock powder with 1N HCl for 6 hours. Pb from both types of treatments was purified on 0.5 ml quartz glass columns charged with DOWEX AG 1x8 anion exchange resin, using a mixed HBr–HCl elution chemistry. The procedure blank amounted to ~ 300 pg total Pb. U and Pb from the dissolved U-rich minerals were separated on miniaturized 150 µl Teflon columns applying the same reagents as for the bulk rock samples. This procedure resulted in a blank of ~ 45 pg total Pb. U was purified using HNO_3 on the same column. The purified Pb samples were dissolved in a silica gel-phosphoric acid mixture and subsequently transferred to 20 µm Re filaments. Pb analyses were carried out using a VG Sector mass-spectrometer. U was analyzed in a triple Ta–Re–Ta filament setting on a single cup AVCO mass spectrometer. For this the samples were dissolved in 0.1 N HNO_3 and loaded on both laterally positioned Ta filaments. Fractionation of the NBS 981 Pb standard amounted to 0.85 ± 0.13 per mil /AMU (n = 85). Errors of the measured Pb isotope ratios are reported at the 1σ level and are corrected for fractionation and blank contribution. All age errors in this paper are reported on a 1σ level.

3. Results and discussion

3.1. MINERALOGY OF U IN REDUCTION SPOT CORES AND CHEMICAL AGES BASED ON MICROPROBE ANALYSES

In the mineralized reduction spots pitchblende (uraninite) and coffinite are common whereas brannerite, uraniferous leucoxene and an unidentified U-As-oxide mineral are less abundant. The diameter of optically homogeneous grains of uraninite, which is usually the largest mineral, never exceeds 50 to 100 µm, more typical are diameters of 1 to 5 µm. In many samples a substantial amount of uranium occurs in mineral grains < 1 µm in diameter (Fig. 2). Hence, the uranium minerals accessible to single mineral microprobe analysis are not necessarily representative for the bulk of the uranium present in a mineralized core.

Chemical ages of uranium minerals in reduction spots based on microprobe analyses are reported in table 1. Coffinite and brannerite are subject to metamictization and Pb loss from these minerals is indicated by very variable Pb/U ratios, not considered to be age indicators, therefore. Uraninite has a very stable crystal lattice and commonly is not metamictized. Thus, Pb- or U redistribution is less likely. The standard deviation of Pb/U ratios measured at different µm-sized spots within a single mineral grain or a group of petrographically identical grains may be influenced by a number of natural and analytical factors such as grain size, small-scale Pb remobilization without Pb loss, bulk Pb loss and count statistics. Large standard deviations may thus be present while the chemical age may still close to the formation age. Small standard deviations indicate homogeneous Pb distribution and no Pb loss. Ages with smaller standard deviations are more likely, but not necessarily, closer to the formation age, therefore. The influence of nonradiogenic Pb on microprobe-derived Pb/U is considered insignificant based on the incompatibility of Pb in the UO_2 lattice and very low Pb-contents in Tertiary uraninites from Pb-rich environments (HOFMANN and KNILL, 1996).

Tab. 1 U–Pb chemical ages based on microprobe analyses of U-minerals in reduction spot cores.

Sample	Mineral	U wt%	Th wt%	Pb wt%	chemical age [Ma]	± 1σ [Ma]	n *
Rin 819.0	uraninite	67.05	0.02	0.41	43	6	18
Rin 819.0	uraninite	66.13	0.42	0.03	45	4	6
Rin 819.0	uraninite	58.58	0.03	0.42	51	9	5
Rin 819.0	brannerite	28.64	0.07	0.69	183	59	11
Rin 834.0	uraninite	69.06	0.18	0.41	43	16	23
Rin 834.0	uraninite	71.00	0.03	0.81	81	13	11
Rin 867.0	U–As–Si–O	30.53	0.04	0.31	75	21	16
Rin 900.0	uraninite	61.17	0.27	0.40	47	9	15
Rin 908.0	uraninite	69.65	0.03	0.43	43	14	10
Rin 999.0	uraninite	59.05	0.01	0.23	27	11	7
Rin 1639.0 [1]	uraninite	76.45	0.08	1.47	135	25	6
Rin 1639.0	uraninite	65.34	0.52	1.23	135	7	6
Rin 1639.0 [1]	brannerite	40.48	0.00	0.55	96	30	6
Rin 1639.0	brannerite	38.30	0.25	0.50	96	28	3
Kai 145.0	uraninite	70.40	0.07	1.46	146	33	7
Kai 208.7	uraninite	74.33	0.02	1.13	108	11	5
Kai 351.0	U–As–O	64.08	0.44	0.07	8	5.6	21
Wei 1038.6	uraninite	74.38	0.01	0.42	40	14	10
Wei 1043.0	uraninite	74.42	0.06	1.42	148	21	6
Wei 1043.0	uraninite	72.46	0.01	0.52	49	7	5
Wei 1046.0	uraninite	70.92	0.03	0.41	41	10	17
Wei 1076.0 [1]	uraninite	79.60	0.00	1.68	138	12	8
Wef 125	uraninite	61.23	0.07	1.22	140	6	3
Wef 245	uraninite	55.46	0.02	0.18	23	9	14
Wef 245 [1]	uraninite	66.73	0.03	1.08	113	67	6

[1] data from HOFMANN (1990)
* number of spot analyses

A histogram of the superimposed chemical ages of analyzed uraninites based on the data of table 1 is presented in figure 4. Two probability maxima at 138 and 45 Ma are evident. Based on Chi-square testing, only the single value of 108 ± 11 Ma cannot be ascribed to two normal distributions. We believe that the maximum at 138 Ma reflects the primary formation age, with limitations set by unknown common Pb content and possible radiogenic Pb loss. The maximum at 45 Ma may be either due to continuous or episodic Pb loss or may represent a second event of pitchblende generation or -recrystallization during the Tertiary. A Tertiary event might be related to increased heat flow and/or Tectonics in context with the uplift of the Schwarzwald and subsidence of the Rhinegraben as is reflected, e.g., in the Krunkelbach uranium deposit (HOFMANN and EIKENBERG, 1991).

The uraninites yielding the higher ages are often significantly coarser grained than those of the lower age group. Both types of ages were obtained from all boreholes and even in single samples (e.g. Wei 1043.0, Wef 245). Based on microscopic examination, samples Rin 1639.0 (135 ± 7 Ma, HOFMANN, 1990 reported 135 ± 25 Ma based on analyses with an ARL-SEMQ microprobe) and Wei 1076.0 (138 ± 12 Ma) appear the most reliable and are identical within error with the peak of the frequency distribution (Fig. 4). In the first sample, uraninite occurs as partly idiomorphic crystallites up to 5 μm in size. In the latter, uraninite occurs as botryoids up to 20 μm in the smallest dimension and is fully enclosed in organic material (HOFMANN, 1993).

Th concentrations in all investigated uranium minerals are very low with an average Th/U ratio of 0.0023 ± 0.0020. One sample (Kai 351.0) represents an exception (Th/U = 0.007), as was already established in previous work with an independent method (HOFMANN, 1991b).

3.2. BULK LEAD GEOCHEMISTRY IN REDUCTION SPOTS

Pb-analyses of six pairs of redbed host rocks and reduction spot haloes from northern Switzerland and from nearby SW Germany (Tab. 2) show that

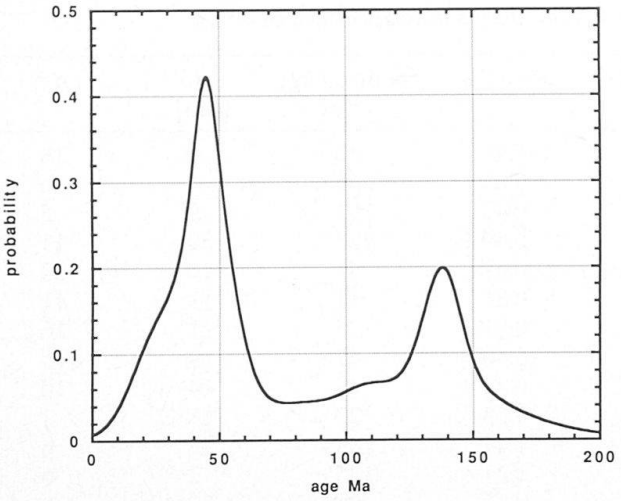

Fig. 4 Histogram of chemical U–Pb ages obtained by superimposing normal distributions of age probability for the 20 uraninite samples listed in table. 1. All samples are from the Permian of northern Switzerland.

Tab. 2 Comparison of Pb and Fe concentrations in red beds and reduction spot haloes.

Sample	Pb ppm	Pb loss %	Fe wt%	Fe loss %
Mumpf red beds	26.5		2.77	
Mumpf halo	10.0	62.3	0.63	77.3
Weierfeld red bed	26.0		4.44	
Weierfeld halo	8.9	65.8	2.01	54.7
Weitenau red bed	40.0		5.16	
Weitenau halo	11.1	72.3	2.68	48.1
Kai 208.6 red bed	46.8		n.a.	
Kai 208.6 halo	18.1	61.3	n.a.	
Kai 214.9 red bed	51.2		n.a.	
Kai 214.9 halo	21.9	57.2	n.a.	
Kai 230.0 red bed	48.0		4.55	
Kai 230.0 halo	28.0	41.7	2.84	37.6

n.a. = not analyzed

haloes are systematically depleted in Pb by 60 ± 10%. The mobility of Pb in reduction spot haloes is similar to that of Fe (Tab. 2) while no other elements are significantly depleted in the haloes (HOFMANN, in prep.). The depletion of Fe is best explained by reductive dissolution of ferric (hydr)oxides and subsequent diffusive transport. The associated Pb depletion may result from dissolution of ferric oxides possibly acting as Pb carrier phases. In the mineralized reduction spot cores, Pb occurs in several minerals. We assume that the Pb present in these minerals is part of the Pb mobilized during halo formation. Clausthalite (PbSe) is abundant whereas altaite (PbTe) and galena (PbS) are rare. Mass balance calculations for the reduction spots Kai 208.61 and Kai 214.96 suggest that the Pb present in the mineralized cores corresponds to about 5% of the Pb mobilized from haloes. The amount of Pb mobilized from reduction spots corresponds to a bulk rock pore fluid Pb content of 10–20 ppm assuming 6 vol.% haloes in bulk rock (HOFMANN, 1990). While the amount of Pb mobilized from the bulk rock is significant, the site of re-precipitation is uncertain.

Tabl. 3 U–Pb data for U mineralized reduction spot cores from Permian red beds, Northern Switzerland. Due to the heterogeneity of mineralized reduction spots, the analyses are not representative for whole mineralized spots

Sample (number = depth)	borehole	weight [mg]	$^{206/204}$Pb (measured)	U (%)	Pb rad (ppm)	Pb rad (%)	206/207 (calculated*)	235/207 (calculated*)	207/235 [Ma]**	206/238 [Ma]**	207/206 [Ma]**
Rin 819	Riniken	3.61	20.39	3.07	196.0	6.5	1.71	5.38	173.0	14.8	4470
Rin 834b	Riniken	22.44	35.32	0.76	16.6	19.4	13.95	43.41	23.1	15.0	977
Rin 835	Riniken	0.74	29.35	6.73	76.4	13.2	17.75	104.54	9.7	7.9	465
Rin 867b	Riniken	13.13	21.40	0.42	9.2	7.6	2.50	16.67	59.2	7.0	3910
Rin 1639	Riniken	0.33	60.37	12.20	407.0	36.5	17.20	33.57	29.8	23.9	535
Kai 162.9	Kaisten	4.53	24.71	4.07	6.8	8.4	7.73	329.27	3.1	1.1	2090
Kai 214.9	Kaisten	3.38	21.61	0.87	22.9	3.6	16.06	37.27	26.9	20.1	685
Kai 351	Kaisten	0.65	22.88	0.95	13.1	6.0	12.12	64.05	15.7	8.8	1257
Wei 1043.8	Weiach	0.63	21.36	5.01	39.6	4.2	4.72	47.52	21.2	4.6	2920
Wei 1046.4	Weiach	3.66	31.36	5.24	4.1	16.0	8.49	758.73	1.3	0.5	1924

* Common Pb correction: average whole rock Pb of Kai 208.61 and Kai 214.96, corrected back to 120 Ma: $^{206/204}$Pb = 18.668, $^{207/204}$Pb = 15.701.

** no errors reported because uncertainty due to common Pb correction larger than analytical error.

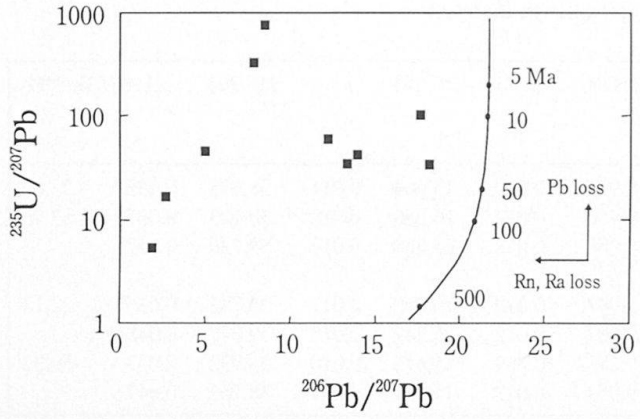

Fig. 5 $^{206}Pb/^{207}Pb$ versus $^{235}U/^{207}Pb$ plot (adopted from LUDWIG and SIMMONS, 1992) of U-mineralized reduction spot samples from northern Switzerland. All samples are highly discordant with indications of loss of both ^{238}U short lived daughter elements and radiogenic Pb. The concordia is shown with reference age points in Ma.

3.3. U–Pb DATING OF U-RICH CORES, LEAD MINERALS

U–Pb data of U-mineralized reduction spot cores are presented in table 3 and figure 5. All samples are highly discordant with $^{207}Pb/^{206}Pb$ of 0.03–0.56 corresponding to "ages" of up to 4.7 Ga indicating a large loss of ^{238}U daughters. ^{235}U–^{207}Pb ages, assumed to be least affected by daughter element migration, are largely Tertiary and possibly indicate an event of Pb mobilization or uraninite recrystallization during this time. The U-content of the analyzed samples ranged from 0.4 to 12.2%, indicating the presence of approximately 0.6 to 18% uraninite.

Pb isotope data of clausthalite (PbSe) from cores of reduction spots are presented in table 4 together with U–Th–Pb data of haloes and host rocks. This Pb is significantly more thorogenic than the inferred bulk rock Pb initial (see 3.5.), indicating that Pb mobilized from haloes and partially fixed as clausthalite in the cores of reduction spots was enriched in radiogenic Pb when compared to that present in the bulk rock.

3.4. LEAD ISOTOPE SYSTEMATICS OF BLEACHED HALOES AND HOST ROCKS

In figure 6 a, b Pb isotope ratios of red host rocks, bleached haloes, Pb minerals (clausthalite) and a whole rock leach are presented. Pb isotope ratios from the halo are more radiogenic than those from the host rocks. A halo-red bed tie-line with bulk rock samples in the $^{207}Pb/^{204}Pb$–$^{206}Pb/^{204}Pb$ plot (Fig. 6a) corresponds to a $^{207}Pb/^{206}Pb$ ratio of 0.036, which results in a negative age. This clearly indicates that ^{206}Pb, but not ^{207}Pb, has been added from migrating intermediary daughter elements of ^{238}U, consistent with the inferred loss of ^{238}U

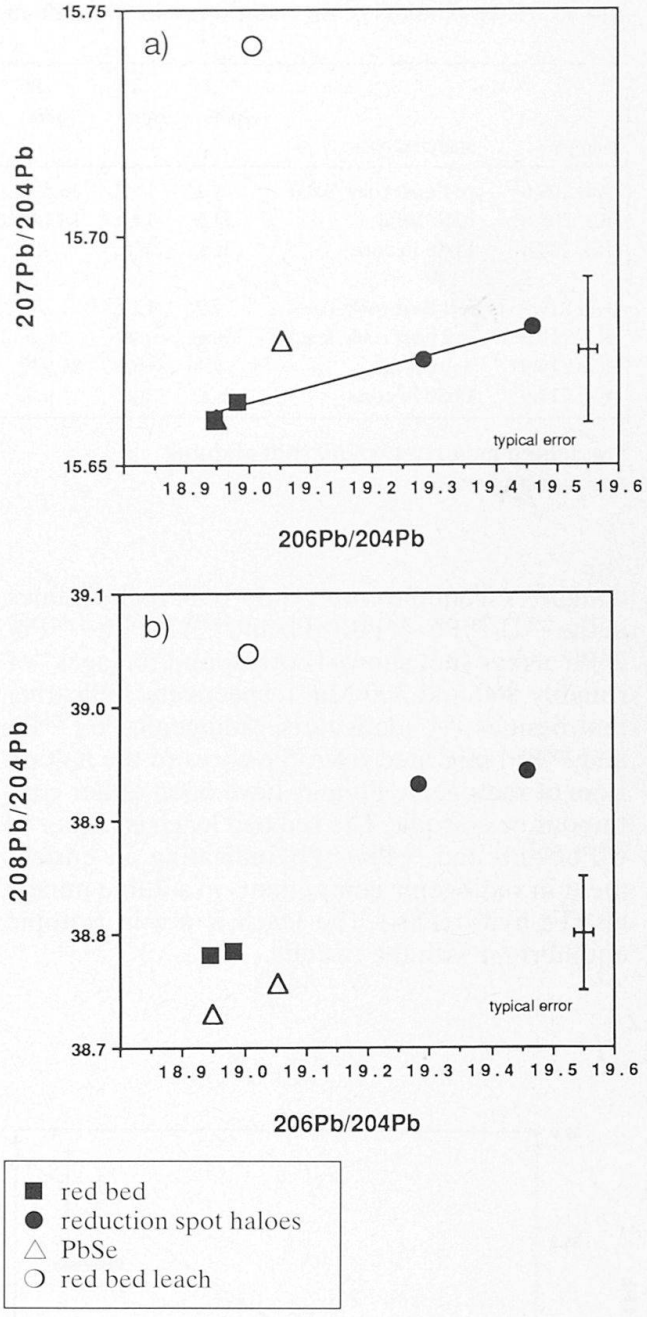

Fig. 6 Pb–Pb plots for red bed and halo total Pb, red bed leach and clausthalite in samples Kai 208.6 and Kai 214.9.
a) $^{206}Pb/^{204}Pb$ versus $^{207}Pb/^{204}Pb$. A slope of 0.036 defined by red bed- and halo samples (filled symbols) corresponds to a negative $^{207}Pb/^{206}Pb$ age, indicating selective ^{206}Pb-enrichment due to mobilization from cores to haloes.
b) $^{206}Pb/^{204}Pb$ versus $^{208}Pb/^{204}Pb$. Note enrichment of thorogenic Pb in haloes.

Tab. 4 U–Th–Pb data of the main zones in two reduction spots from Kaisten

Sample	analyzed phase	U (ppm)	Th (ppm)	Pb (ppm)	206/204	± 1 σ	207/204	± 1 σ	208/204	±1 σ	$^{232}Th/^{204}Pb$
Kai 208.6*	red host rock, total	7.1	16.2	46.826	18.984	0.010	15.664	0.011	38.785	0.035	23.00
Kai 208.6*	halo, total	21.8	14.6	18.146	19.460	0.012	15.680	0.012	38.943	0.037	53.96
Kai 208.6	PbSe in core	n.a.	n.a.	n.a.	18.950	0.012	15.660	0.014	38.730	0.047	
Kai 214.9*	red host rock, total	7.2	17.1	51.248	18.947	0.010	15.660	0.011	38.782	0.035	22.17
Kai 214.9	red host rock, leach	n.a.	n.a.	n.a.	19.007	0.012	15.742	0.015	39.047	0.048	
Kai 214.9*	halo, total	7.1	16.5	21.935	19.285	0.009	15.673	0.010	38.932	0.033	50.32
Kai 214.9	PbSe in core	n.a.	n.a.	n.a.	19.054	0.012	15.677	0.014	38.757	0.047	

* weighted mean of two dry split aliquots
n.a.: not analyzed

daughters from the cores. Halo-bulk rock tie lines in the $^{238}U/^{204}Pb$–$^{206}Pb/^{204}Pb$ and $^{235}U/^{204}Pb$– $^{207}Pb/^{204}Pb$ arrays (not shown) correspond to "ages" of roughly 800 and 500 Ma, respectively, indicating that besides ^{238}U daughters, radiogenic Pb (^{206}Pb and ^{207}Pb) migrated from the cores to the haloes. Loss of radiogenic Pb may have been either continuous or episodic. The red bed leach is higher in $^{207}Pb/^{204}Pb$ and $^{208}Pb/^{204}Pb$, indicating an enrichment in radiogenic components in soluble minerals (Fe-hydroxides). The leach is not in isotopic equilibrium with the residue.

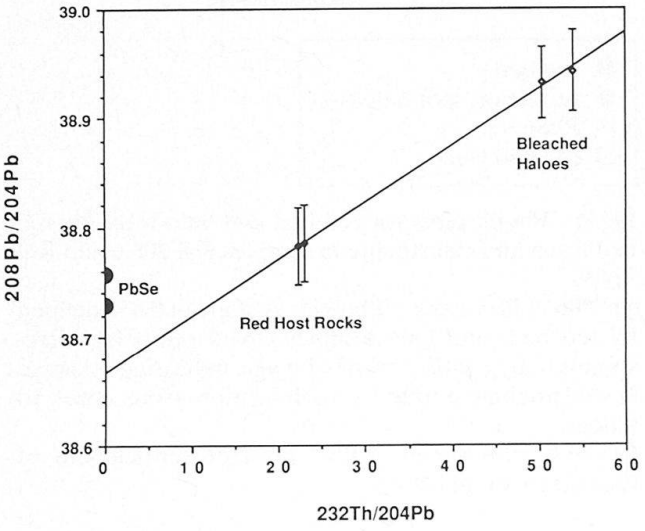

Fig. 7 ^{232}Th–^{208}Pb isochron plot for two pairs of haloes and host rocks (Kaisten 208.6 m and 214.9 m). The slope is 0.0052 ± 6 yielding an age of 105 ± 12 Ma. Also plotted are clausthalite (PbSe) lead isotope data for the same spots. Error in $^{232}Th/^{204}Pb$ is 2% (similar to symbol size).

3.5. Th–Pb DATING OF BLEACHED HALOES AND HOST ROCKS

Bleached haloes have significantly higher Th/Pb ratios than bulk rocks because they are strongly depleted in Pb while Th concentrations were not affected. This allows, in principle, for the determination of ^{232}Th–^{208}Pb (minimum) ages of halo formation, or, more precisely, of Pb depletion. This approach was used on two host rock-halo pairs from two reduction spots (Kai 208.6 m, Kai 214.6 m). Data are presented in table 4 and in a $^{232}Th/^{204}Pb$–$^{208}Pb/^{204}Pb$ (isochron) plot (Fig. 7). The slope of the isochron yields an age of 105 ± 12 Ma. Any value obtained by this method represents a minimum age because selective leaching of radiogenic Pb isotopes from the halo during Pb depletion is likely, resulting in an initially negative slope of the isochron. For this reason, the $^{208}Pb/^{204}Pb$ ratio probably was slightly lower in the halo than in the bulk rock just after halo formation. Possible deposition of mobilized Pb in the red bed surrounding the halo is considered to be quantitatively insignificant based on mass balance calculations.

The large error of the slope, due to the limited spread of Th/Pb ratios, precludes close age constraints. However, based on these data a Cretaceous age of halo formation is probable. The feasibility of a ^{232}Th–^{208}Pb approach to date red bed bleaching phenomena is demonstrated. Immobility of Th is confirmed by the low concentration of this element in the analyzed U minerals from reduction spots in the Permian. Core material of sample Kai 214.96, analyzed for Th by ICP-MS yielding 13.0 ppm (host rock 17.1 ppm), clearly shows that Th was not enriched but rather diluted because of the addition of other elements.

4. Conclusions

The U–Pb isotopic system of reduction spots is characterized by significant loss of daughter elements of ^{238}U (perhaps ^{226}Ra and ^{222}Rn) as well as of total radiogenic Pb. Daughter element loss is most likely facilitated by the extremely small grain size (< 1 μm) of the bulk of the uranium minerals (Fig. 2). Additionally, high concentrations of common Pb are present, typically as clausthalite. The primary age of reduction spot formation is not preserved by the U–Pb system with only one sample showing a Mesozoic $^{235}U/^{207}Pb$ age. Near concordant Tertiary ages may indicate an event of radiogenic Pb mobilization or uraninite recrystallization. Chemical ages based on microprobe analyses of selected large grains of uraninite appear to be least disturbed and define two age groups near 138 and 45 Ma, demonstrating that grain size is an important factor for daughter element. Loss of about 50% of the rock's Pb from the bleached haloes results in an increase of $^{232}Th/^{208}Pb$ ratios in bulk rocks from 20–25 to 50–55, allowing the determination of $^{232}Th/^{208}Pb$ minimum ages. This dating approach may be applicable to red bed bleaching in general provided that Pb mobilization is a feature not restricted to reduction spots.

The absolute age of the investigated reduction spots probably is Lower Cretaceous based on consistent, but partially imprecise data: the lowest K–Ar roscoelite age is 112 ± 2 Ma (HOFMANN, 1990), the higher probability maximum of chemical U–Pb ages is 138 Ma, and the ^{232}Th–^{208}Pb age is 105 ± 12 Ma. The depth of burial in the Lower Cretaceous was at least 1000 m (Kaisten) and up to 2000 m for the deeper Riniken samples. Whether reduction spot formation was related to a regional thermal or tectonic activity is unknown, but the abundance of Mesozoic ages of hydrothermal mineralizations in the Black Forest area indicates that reduction spot formation and large scale mineralization events may have been coeval. Many mineralizations in the Black Forest area have post-Permian ages ranging from 240 to 50 Ma (BONHOMME et al., 1983; MERTZ, 1987; KIRSCH, 1989; HOFMANN and EIKENBERG, 1991; LIPPOLT and SIEBEL, 1991; MERTZ et al., 1991; SEGEV et al., 1991; KARPENKO et al., 1993; HAGEDORN and LIPPOLT, 1994; LIPPOLT and KIRSCH, 1994; WERNICKE and LIPPOLT, 1993, 1994, 1995). K-Ar-dating of Carboniferous and Permian sediments from the Weiach well (SCHALTEGGER et al., 1995) yielded evidence of an event at 183 ± 5 Ma in northern Switzerland. Whether the regionally common Mesozoic ages represent several distinct mineralizing events or continuous hydrothermal activity is unknown. The results presented in this paper demonstrate that the U–Th–Pb system of small-scale redox systems (reduction spots) from northern Switzerland is complex and disturbed. As the majority of U is present in μm-sized mineral grains in reduction spot cores, these are not closed systems for uranium daughters and preclude dating by conventional U–Pb isotopic methods.

Acknowledgements

This study is part of a wider project on redox processes supported by Nagra (Swiss National Cooperative for Radioactive Waste Disposal) which also provided the samples. We thank H. Oschidari and R. Maeder for XRF- and AAS analyses. The electron microprobe of the Mineralogisch-petrographisches Institut at the University of Bern is supported by the Swiss National Science Foundation (grant 21-26579.89). Constructive reviews by R.S. Wernicke, U. Schaltegger, R. Alexander and an anonymous reviewer helped to improve the manuscript.

References

BONHOMME, M.G., BAUBRON, J.-C. and JEBRAK, M. (1987): Minéralogie, géochimie, terres rares et âge K–Ar des argiles associées aux minéralisations filoniennes. Chem. Geol. (Isot. Geosc. Sect.) 65, 321–339.

BOWLES, J.F.W. (1990): Age dating of individual grains of uraninite in rocks from electron microprobe analyses. Chem. Geol. 83, 47–53.

CARTER, G.E.L. (1931): An occurrence of vanadiferous nodules in the Permian beds of South Devon. Mineral. Mag. 22, 609–613.

CURIALE, J.A., BLOCH, S., RAFALSKA-BLOCH, J. and HARRISON, W.E. (1983): Petroleum-related origin for unraniferous organic-rich nodules of southwestern Oklahoma. Bull. Amer. Assoc. Petroleum Geol. 67, 588–608.

DIEBOLD, P., NAEF, H. and AMMANN, M. (1992): Zur Tektonik der zentralen Nordschweiz. Nagra (Natl. Coop. Disposal Radioactive Waste) Technical Report 90–04, 277 pp.

HAGEDORN, B. and LIPPOLT, H.J. (1994): Isotopische Alter von Zerrüttungszonen als Altersschranken der Freiamt-Sexau-Mineralisation (Mittlerer Schwarzwald). Abh. Geol. Landesamt Baden-Württemb. 14, 205–219.

HARRISON, R.K. (1975): Concretionary concentrations of the rarer elements in Permo-triassic red beds of south-west England. Bull geol. Surv. G.B. 52, 1–26.

HOFMANN, B. (1989): Genese, Alteration und rezentes Fliess-System der Uranlagerstätte Krunkelbach (Menzenschwand, Südschwarzwald). Nagra (Natl. Coop. Disposal Radioactive Waste), Tech. Rep., 88–30, 195 pp.

HOFMANN, B.A. (1990): Reduction spheroids from northern Switzerland: Mineralogy, geochemistry and genetic models. Chem. Geol. 81, 55–81.

HOFMANN, B.A. (1991a): Mineralogy and geochemistry of reduction spheroids in red beds. Mineral. Petrol. 44, 107–124.

HOFMANN, B.A. (1991b): A uranium series disequilibrium investigation of reduction spheroids in red beds. Schweiz. Mineral. Petrogr. Mitt. 71, 333–340.

HOFMANN, B.A. (1992): Isolated reduction phenomena in red beds: A result of porewater radiolysis? In: KHARAKA, Y.K. and MAEST, A.S. (eds): Water-Rock Interaction. Balkema, Rotterdam, 503–506.

HOFMANN, B.A. (1993): Organic matter associated with mineralized reduction spots in red beds. In: PARNELL, J., KUCHA, H., LANDAIS, P. (eds): Bitumens in ore deposits (Springer), 362–378.

HOFMANN, B. and EIKENBERG, J. (1991): The Krunkelbach Uranium Deposit, Schwarzwald, Germany: Corrleation of Radiometric Ages (U–Pb, U–Xe–Kr, K–Ar, ^{230}Th–^{234}U) with Mineralogical Stages and Fluid Inclusions. Econ. Geol. 86, 1031–1049.

HOFMANN, B.A. and KNILL, M.D. (1996): Geochemistry and genesis of the Lengenbach Pb-Zn-As-Tl-Ba-mineralisation, Binn Valley, Switzerland. Mineralium Deposita 31, 319–339.

KARPENKO, M.I., IVANENKO, V.V., MERTZ, D.F. and LIPPOLT, H.J. (1993): A Laser ^{39}Ar–^{40}Ar Method for Dating Authigenic Adularia Microcrystals. Geochem. Intl. 30, 121–125.

KIRSCH, H. (1989): $^{40}Ar/^{39}Ar$-chronologische und mineralogische Untersuchungen zur Sericitisierung von Plagioklasen. Unpublished Ph. D. Thesis, University of Heidelberg, 232 pp.

LIPPOLT, H.J. and KIRSCH, H. (1994): Isotopic investigations of Post-Variscan Plagioclase Sericitization in the Schwarzwald Gneiss Massif. Chemie d. Erde 54, 179–198.

LIPPOLT, H.J. and SIEBEL, W. (1991): Evidence for multistage alteration of Schwarzwald lamprophyres. Europ. J. Mineral. 3, 587–601.

LUDWIG, K.R. and SIMMONS, K.R. (1992): U–Pb dating of uranium deposits in collapse breccia pipes of the Grand Canyon Region. Econ. Geol. 87, 1747–1765.

LUDWIG, K.R., GOLDHABER, M.B., REYNOLDS, R.M. and SIMMONS, K.R. (1982): U–Pb isochron age and preliminary sulfur isotope systematics of the Felder uranium deposit, south Texas. Econ. Geol. 77, 557–563.

LUDWIG, K.R., SIMMONS, K.R. and WEBSTER, J.D. (1984): U–Pb isotope systematics and apparent ages of uranium ores, Ambrosia Lake and Smith Lake districts, Grants mineral Belt, New Mexico. Econ. Geol. 79, 322–337.

MATTER, A. (1987): Faziesanalyse und Ablagerungsmilieus des Permokarbons im Nordschweizer Trog. Eclogae geol. Helv. 80, 345–367.

MATTER, A., PETERS, TJ., ISENSCHMID, CH., BLÄSI, H.-R. and ZIEGLER, H.-J. (1988a): Sondierbohrung Riniken. Geologie. Nagra (Natl. Coop. Disposal Radioactive Waste) Technical Report 86-02, 198 pp.

MATTER, A., PETERS, TJ., BLÄSI, H.-R., Meyer, J., ISCHI, H., MEYER, CH. and ZIEGLER, H.-J. (1988b): Sondierbohrung Weiach. Geologie. Nagra (Natl. Coop. Disposal Radioactive Waste) Technical Report 86-02, 438 pp.

MAW, G. (1868): On the disposition of iron in variegated strata. Quart. J. geol. Soc. London 24, 351–400.

MEMPEL, G. (1960): Neue Funde von Uran-Vanadiumkernen mit Entfärbungshöfen: Geol. Rdsch. 49, 263–276.

MERTZ, D.F. (1987): Isotopengeochemische und mineralogische Untersuchungen an postvariscischen hydrothermalen Schichtsilikaten. Unpublished Ph. D. Thesis, University of Heidelberg, 207 pp.

MERTZ, D.F., KARPENKO, M.I., IVANENKO, V.V. and LIPPOLT, H.J. (1991): Evidence for Jurassic Tectonism in the Schwarzwald Basement (SW Germany) by Laser Probe $^{40}Ar/^{39}Ar$ Dating of Authigenic K-feldspar. Naturwissenschaften 78, 411–413.

PERUTZ, M. (1940): Radioactive nodules from Devonshire, England. Schweiz. Mineral. Petrogr. Mitt. 20, 141–161.

PETERS, TJ., MATTER, A., ISENSCHMID, CH., MEYER, J. and ZIEGLER, H.-J. (1989): Sondierbohrung Kaisten. Geologie. Nagra (Natl. Coop. Disposal Radioactive Waste) Technical Report 86-04, 286 pp.

PETERS, TJ., MATTER, A., BLÄSI, H.-R. and GAUTSCHI, A. (1989): Sondierbohrung Böttstein. Geologie. Nagra (Natl. Coop. Disposal Radioactive Waste) Technical Report 85-02, 207 pp.

SCHALTEGGER, U., WINGMANN, H., CLAUER, N., LARQUÉ, P. and STILLE, P. (1995): K–Ar dating of a Mesozoic hydrothermal activity in Carboniferous to Triassic clay minerals of northern Switzerland. Schweiz. Mineralog. Petrogr. Mitt. 75, 163–176.

SEGEV, A., HALICZ, L., LANG, B. and STEINITZ, G. (1991): K–Ar dating of manganese minerals from the Eisenbach region, Black Forest, southwest Germany. Schweiz. Mineral. Petrogr. Mitt. 71, 101–114.

TANTON, T.L. (1948): Radioactive nodules in sediments of the Sibley Series, Nipigon, Ontario: Trans. R. Soc. Can. 17, Ser. III, Sec. 4, 69–75.

WERNICKE, R.S. and LIPPOLT, H.J. (1993): Botryoidal hematite from the Schwarzwald (Germany): heterogeneous uranium distributions and their bearing on the helium dating method. Earth and Planet. Sci. Lett. 114, 287–300.

WERNICKE, R.S. and LIPPOLT, H.J. (1994): Dating of vein specularite using internal $(U+Th)/^{4}He$ isochrons. Geophys. Res. Lett. 21, 345–347.

WERNICKE, R.S. and LIPPOLT, H.J. (1995): Direct isotope dating of a Northern Schwarzwald qtz-ba-hem vein. N. Jb. Miner. Mh. Jg. 1995, H. 4, 161–172.

Manuscript received November 6, 1995; revision accepted May 15, 1996.